STUDY OF A WIND TUNNEL JET ENCLOSURE, DESIGNED TO SIMULATE FREE AIR CONDITIONS

A THESIS

SUBMITTED FOR THE DEGREE

OF

MASTER OF SCIENCE IN AERONAUTICAL ENGINEERING

BY

PENN EVANS MULLOWNEY

Atlanta, Georgia.
Daniel Guggenheim School of Aeronautics
Georgia School of Technology
May 6, 1935

Approved:

STUDY OF A WIND TUNNEL JET ENCLOSURE DESIGNED TO SIMULATE FREE AIR CONDITIONS

Summary

Theories of wind tunnel wall interference and their experimental verifications have been satisfactorily compared at present for all practical types of jet shapes and jet-boundaries. Prandtl's suggested use of a doubly infinite arrangement of airfoil images for a rectangular jet induced Glauert and later Theodorsen to complete the theory, based on slightly differing assumptions, for this shape of jet with several different types of boundaries.

This report presents the results of square-jet wind tunnel tests carried out at the Georgia School of Technology with a series of jet-boundaries which were partly open and partly closed. The longitudinal openings or slots of the boundaries were alternated completely around the jet with the longitudinal closures or slats. It was thus possible to determine the percentage of jet closure, constructed in this manner, that would produce a zero jet-boundary correction factor for this certain shape of tunnel. It was found that the boundary would have to be almost completely closed to obtain this correction factor, or to simulate the infinite airstream of free-air conditions for the square tunnel.

Introduction

In the past ten years a certain group of investigators have attacked the problem of corrections to experimental airfoil test results made necessary by the presence of the wind tunnel boundary and its interference. Prandtl in 1921 inaugurated the basic theory for a wind tunnel of circular cross-section which was later extended by others to embrace practically all shapes of jets.

Prandtl's theory was derived from the assumptions that the conditions of the airflow in a wind tunnel are such that there is zero flow normal to a rigid boundary surrounding a model in a closed tunnel, and zero change in pressure normal to the imaginary cylinder about the undisturbed airstream of a free jet. However, if a model were tested in either of the above tunnels, the forces produced would not be the same as those that would be produced if the model had been in an airstream of infinite extent. To determine mathematically the amount of the corrections that must be applied to experimental results obtained in a jet of finite dimensions, it was necessary to construct a system which would produce the boundary conditions that exist about such a jet, and, this being effected, to calculate the induced flow at the airfoil caused by the system. As a mathematical device, image vortices were placed outside the rigid or imaginary tunnel walls in the plane of the airfoil tip vortices and symmetrically along the line of the model span. The strengths of these vortices were equal to that of the horse-shoe system of the airfoil, and the directions were such that the boundary conditions would be reproduced at every point. The problem then resolved into a calculation of the velocity at the center of the airfoil span, the change in angle of attack, and the change in drag induced by these vortices. These changes appeared in terms of airfoil and tunnel dimensions, of the lift coefficient, and of some constant δ, depending on the shape of the jet. It was found that an upward inclination of the airstream and corresponding decrease in drag resulted from the presence of the solid boundaries, and that a downward deflection of the airstream with increase in drag was the result of the free-jet boundaries. Thus the changes in angle of attack, $\Delta\alpha$, and in drag, ΔC_D, and the correction factors, δ, would have positive signs for the closed tunnel and negative for the free jet. Theoretically, these increments with the proper signs would bring the test results to values that would be obtained if the model had been tested in an infinite airstream.

Prandtl's device of using external image vortices was extended to the case of an infinitesimal airfoil in a closed rectangular tunnel by Glauert (Refs. 1,2, and 3). Terazawa and Rosenhead (Refs. 4 and 5) extended the theory to include airfoils of finite span. Theodorsen (Ref. 6) produced a very interesting general theory for small spans in four other types of rectangular tunnels, one being the open or free jet, and three being partly open, partly closed with alternate plane boundaries extending entirely across the sides of the jet. He also produced results (Ref. 7) for the case of a finite airfoil in an open rectangular jet. Meanwhile, Sanuki and Tani (Ref. 8) and Rosenhead (Ref. 9) investigated the case of airfoils in a wind tunnel of elliptic cross-section. Glauert

(Ref. 10) published recently a comprehensive summary of the theories of interference on bodies tested in all practical shapes of wind tunnels.

Experimental justifications of several of these theories have been carried out. Cowley and Jones (Ref. 11) and Higgins (Ref. 12 and 13) tested Prandtl's original correction factors. Knight and Harris (Ref. 14) obtained good results using Prandtl's factor as calculated by Glauert (Ref. 15) for the circular and rectangular open tunnels. Theodorsen (Ref. 16), attempting to verify his prediction that there were at least three partly open, partly closed types of rectangular jets that would produce free air conditions for certain ratios of tunnel jet height-to-width ratios (designated as λ throughout this report), tested airfoils in the model of the full-scale oval-throat tunnel of the National Advisory Committee for Aeronautics which was altered to give various conditions of rectangular boundaries. Schliestett, using the small square-section jet at the Georgia School of Technology, made tests considering all five cases of Theodorsen's jet boundary conditions. His results are given in Reference 17.

Theodorsen originally predicted free air conditions, or correction factor $\delta = 0$, for airfoils of very small span, in a square jet with horizontal boundaries, in a rectangular tunnel of $\lambda = .5$ with vertical boundaries, and in a rectangular tunnel of $\lambda = .5$ with one horizontal boundary only. It was later stated that a square jet with vertical boundaries would maintain free air conditions. However, Schliestett has shown by experimental tests and by certain corrections to Theodorsen's analysis, that for a rectangular tunnel with vertical boundaries, a zero correction factor exists for $\lambda = 2$. The corrected curves of correction factor δ, versus λ, the ratio of tunnel jet height to width, as presented in Figure 1, have been agreed to by Theodorsen. Thus, for the square tunnel, there is only one simple arrangement of the jet boundaries that will represent free air conditions, and this is effected by the use of horizontal boundaries.

From a study of Figure 1, it can be seen that, although there is no rectangular open or closed jet that will produce free air conditions, a square jet 50 percent closed with the boundaries above and below the model will satisfy the conditions, and a square jet 50 percent closed but with the boundaries at the sides of the model will not, although the correction is less than, but of the same sign, as that of the free jet. It would be desirable from a practical standpoint to be able to use similar systems of jet boundaries for every shape of wind tunnel jet. It could be expected, from Theodorsen's analysis, that a partly open, partly closed system of boundaries, arranged so that the openings were uniform about all four sides, would produce the desired conditions, for the square jet, and with some particular ratio of jet boundary opening to closure. As a beginning, an experimental investigation of a system of jet boundaries that would also simulate the free air conditions in a tunnel of arbitrary and finite dimensions (square tunnel) was carried out. It is the purpose of this report to present the results of an investigation of empirically constructed jet boundaries, formed of alternating slots and slats parallel to the airstream, showing the effect of such boundaries constructed about a square jet.

Force tests were made in the small wind tunnel of the Georgia School of Technology, with boundaries open and closed, and of four ratios of slat closure to slot opening as follows:

I.	Free Jet (Open Tunnel)		- Zero closure
II.	Boundaries with Slat/Slot Ratio	1:1	- 50 percent closure
III.	Boundaries with Slat/Slot Ratio	2:1	- 66.7 " "
IV.	Boundaries with Slat/Slot Ratio	5:1	- 83.3 " "
V.	Boundaries with Slat/Slot Ratio	13.5:1	- 93.1 " "
VI.	Closed Jet		- 100 " "

A mathematical analysis of the effects of such jet boundaries as were used in these tests is not attempted here as it is believed that the image vortex system of preceding treatments would present serious difficulties in the basic assumptions.

The author wishes to acknowledge the assistance of Professor Montgomery Knight who suggested this investigation and made helpful comments on the method of its experimental analysis, of Professor W. B. Johns who made valuable mathematical analyses of fundamental jet boundary correction factors, and of Mr. L. B. Rumph, Jr. who aided in some of the experimental work.

Method of Test

Force tests were made using the five boundary arrangements of Cases I,II,III,IV, and VIon a 3 x 18 inch Clark Y airfoil model (span 60 percent of tunnel width) at an average Reynolds Number of 159,000. The tunnel used in all cases had a 2-1/2 foot square jet with the transverse plane of the model suspension point 12 inches downstream from the plane of the entrance cone and 23 inches upstream from the plane of the exit cone. The exit cone is 37-1/2 inches square for the open tunnel, with a bell approximately 9 inches long bringing the area down again to that of 30 inches square. The tunnel is basically of the open-throat closed-return type (Fig. 2). For all except the open tunnel, the boundaries were constructed so that the cross-section of the jet was 30 inches square at all points from the entrance cone to the downstream plane of the exit cone bell.

Lift and drag forces were measured by means of the six-component wire-balance system shown in Fig. 3. The model frame was suspended with piano wire which was as fine as could be allowed for sufficient strength to withstand the maximum loads expected from the largest model tested. The two vertical lift wires (front .016 inch diameter; rear .010 inch diameter) carried the total lift from the model support to the lift balance which was vertically above the model support, but moved upstream slightly so that the lift wires were approximately perpendicular to the airstream. The airstream was found by tests to have an upward deflection of about .4°, depending on the type of boundary used. The lift force was measured directly on the large balance as the sum of the forces in the two lift wires. The drag force was carried upstream along the tunnel centerline, through a horizontal wire (.010 inch diameter), to a point vertically beneath the drag balance, at which point another wire (.010 inch diameter), running upstream and inclined downward at an angle of exactly 45° as measured with a sensitive inclinometer, equalized the drag force in the horizontal and vertical drag wires. Three lateral wires (.010 inch diameter) ran from the model support to the cross-wind balances at the right, and the whole system was kept in initial tension by a counter-weight suspended on another .016 inch diameter wire running downstream and downward to the left from the model support.

The various boundaries were set up by bolting panels, made of longitudinal slats about 3/4 inch in thickness, spaced in the appropriate ratio of closure to opening, to the entrance and exit cones around all four sides of the jet, as shown in Fig. 4. For Case VI, instead of solid walls being used, the basic boundaries, made of adjoining slats 1-1/2 inches wide and sanded smooth on the inner surface, were set up. Boundaries for Cases IV, III, and II were then obtained by taking off, cutting down by 1/2 inch for each case, and replacing alternate slats of the basic closed tunnel boundaries. This produced the jet closures of 83.3 percent, 66.7 percent, and 50 percent for Cases IV, III, and II respectively, since the ratios of slat to slot opening were then 2-1/2": 1/2";

2":1" and 1-1/2":1-1/2". It is to be noted that the cut-down slats of the basic closed tunnel, when replaced to form part of the closure of Cases III and IV, were reset along the centers of the slots from which they were taken, in order to give a more symmetrical distribution of slot opening to slat closure around the boundaries.

The correction factors for drag were obtained from results of force tests in the tunnel with the boundaries of Cases I,II,III,IV, and VI. They were plotted against percent of closure, a smooth curve was drawn through the five points (Fig.5), and a new slatted boundary was constructed which was designed to give the percent of closure for zero-correction or free air conditions with this type of boundary. This represents Case V (Fig. 6 and 7). Final check force tests were run with this boundary, on the 3" x 18" Clark Y, on a 3" x 12" Clark Y, and on a 3" x 24" Clark Y airfoil model to experimentally determine the effect of span on the correction factor, as well as to check the experimentally determined value of percent of closure necessary to produce free air conditions in a squre jet. It was found that his value was given for an approximately 95 percent slotted-closed square jet, as shown later in this discussion.

The three airfoils, 3" x 12", 3" x 18", and 3" x 24", of exact areas 35.55 sq.in., 52.39 sq.in. and 70.80 sq.in., and of aspect ratios 4.06, 6.15, and 8.14 respectively, were made from separate blanks of laminated walnut, shaped to a Clark Y section with an initial tolerance of $\pm$.003 inch in profile. Warping caused fairly uniform twists in the three wings of .05, .10, and 1.0 degree respectively, the twists in the two smaller wings being from center to tips and that in the 24" wing being from tip to tip. The errors produced by these twists in the correction factor δ_D has been shown to be negligible at the high lift coefficients, and they were not compensated in the results, since correction factors near zero lift were not averaged because of large discrepencies from other experimental errors.

Correction factors, δ, are dependent on small differences, ΔC_D and $\Delta \alpha$, between relatively large values of drag coefficient and angle of attack, especially at the values of lift coefficient from about $C_L = .2$ to the extent of the straight-line portion of the angle of attack curves. It was, therefore, necessary to use exceptional care during these tests in making readings of lift, drag, and angle of attack. The overall error of the lift and drag force measurements was in no case greater than 2 percent, but in most cases was kept within 1 percent, since the drag beam-balance was made sensitive by a counterweight and a damping cylinder to $\pm.1$ gram and the lift balance, of the direct reading "Toledo" type with auxiliary damping cylinder, was sensitive to about $\pm$ 3 grams. Readings of angle of attack were made, when possible with the set-up, in the tunnel airstream, by a sensitive inclinometer reading to 1 minute, but in most cases a less sensitive inclinometer, reading to 5 minutes, was necessary.

Static tare readings of the lift and drag balances were found to change with temperature in the tunnel, and it was found necessary to make readings before and after each run, using the final result in most cases. The temperature in the tunnel was observed to increase by as much as 2° to 5° during a run. Although the temperature in the tunnel room was kept as nearly constant as possible, deviations were observed, and the ordinary corrections for variations in dynamic pressure were carried out.

The dynamic pressure was found to vary considerably over the region occupied by the model when the model support was in place. Tests were run (Fig. 8) for each condition of jet boundary, and a mean value of dynamic pressure, integrated over the span of each airfoil used, was obtained. From these values, static plate pressures necessary to maintain the desired dynamic pressure mean value of 87.40 mm. alcohol, over the span of the airfoil, were calculated. These were as follows:

	12" wing	18" wing	24" wing
Case I	84.10	84.46	84.30
Case II		83.04	
Case III		82.44	
Case IV		81.50	
Case V	78.40	79.25	79.30
Case VI		59.46	

The dynamic tare of the model support and wires was found to be affected by the interference of the model as the angle of attack was varied. A further refinement of the results was therefore made by running preliminary dynamic tare force tests on the model support with a dummy 3"x 18" Clark Y airfoil placed in the test position. This airfoil was cut out at the center of its span so that it was not allowed to touch the model support at any time. Tests on the model support were made with this dummy wing both normal and inverted for each boundary condition. The variation of the dynamic tare with angle of attack for Case II is shown in Fig. 9,(See also Figs.5 and 6 of Ref. 17 for results of Case VI in this tunnel).

The upward inclination of the airstream, which was observed to vary with the type of boundary used, was accounted for by making all tests in both the normal and inverted positions, and averaging the results. (Fig. 10)

Results

The following equations were used in reducing the test data to coefficient form:

$$C_L = \frac{L}{q.S}$$

$$C_D'' = \frac{D''}{q.S}$$

$$C_D' = C_D'' - (C_{D_o}'' - C_{D_{o-Ave.}}'')$$

$$\alpha' = \alpha_g - \alpha_{L_o}$$

where the symbols used represent the following:

C_L = absolute lift coefficient.

C_D'' = absolute drag coefficient, uncorrected for jet boundary effect, and unadjusted to the values giving an average drag coefficient **at** zero lift.

C_D' = absolute drag coefficient, uncorrected for jet boundary effect, but adjusted at an average value at zero lift.

C_{D_o}'' = absolute drag coefficient at zero lift for a particular boundary condition.

$C_{D''_{o\text{-Ave.}}}$ = average value of absolute drag coefficients at zero lift for Cases I, II, III, IV, and VI - value for Case I, open tunnel used.

C_D = absolute drag coefficient, corrected for jet boundary effect. Free air drag coefficient.

α' = angle of attack in degrees, measured from zero lift.

α_g = geometric angle of attack, measured in the tunnel with respect to the chord line, and averaged to eliminate the effect of deflection of the airstream.

α_{L_o} = geometric angle of zero lift.

α = angle of attack, corrected for jet boundary effect. Free air angle of attack.

L = measured net lift, not including static and dynamic tares.

D" = measured net drag average of normal and inverted tests, not including static and dynamic tares.

S = area of airfoil.

q = mean dynamic pressure over the span of the model.

The average drag coefficient at zero lift was found to be 0.0186 for the aspect ratio 6 model. The drag curves were adjusted so that all had this value at zero lift (Fig. 11). The curves of lift versus angle of attack were also adjusted so that each had the value $\alpha = 0$ when $C_L = 0$ as shown in Fig. 12.

Turbulence and blocking effects were not considered in these tests.

Experimental jet boundary correction factors were next obtained from these results, using the following equations:

$$\Delta\alpha = \delta_\alpha \cdot \frac{S}{C} \cdot C_L \text{ (in radians)}$$

$$= \delta_\alpha \cdot \frac{180}{\pi} \cdot \frac{S}{C} \cdot C_L \text{ (in degrees)}$$

$$\Delta C_D = \delta_D \cdot \frac{S}{C} \cdot C_L{}^2$$

or:

$$\delta_D = \frac{\Delta C_D}{\frac{S}{C} \cdot C_L{}^2}$$

and $$\delta_\alpha = \frac{\Delta\alpha}{\frac{180}{\pi} \cdot \frac{S}{C} \cdot C_L}$$

where:

$$\Delta C_D = C_D - C_D'$$

$$\Delta\alpha = \alpha - \alpha'$$

δ = the correction factor to be determined.

C = the cross-sectional area of the jet.

The average of the results of Cases I and V are assumed to represent free air conditions, giving C_D and α for a certain lift coefficient. The results for Case V are plotted separately in Fig. 13 along with the free air curves, showing the variation of ΔC_D and $\Delta\alpha$ with aspect ratio.

Analysis of Results

In order to facilitate the computation of the mean correction factors, δ_D and δ_α were plotted versus absolute lift coefficient, for the 18" airfoil (A.R. = 6) in the tunnel with jet boundaries of Cases I,II,III,IV, and VI (Figs. 14 and 15, Tables I-X),for the 12", 18", and 24" airfoils in the tunnel with jet boundaries of Case V (Fig. 16, Tables XI-XVI).

Although, according to all theories advanced thus far, there should be no change in δ with change in lift coefficient, it was found that there was some variation in every case. The curves of Figs. 14,15, and 16 were therefore integrated to obtain the mean values of $\bar{\delta}_D$ and δ_α (Table XVII) and these results were plotted as Fig. 5 which shows the variation in correction factors δ_D and δ_α, with the amount of closure of the horizontally slotted boundaries.

Theodorsen (Ref. 16) has already noted the peculiar behavior of the correction factors when plotted against the lift coefficient and has shown by his experimental results, (Fig. 10 of Ref. 16) that the discrepancies from the theoretical for the angle of attack correction factor are more pronounced than for the drag factor. As shown by the curves of Figs. 14,15, and 16 of this report, the same result has been obtained from these tests. In Fig. 14, it is seen that the correction factor tends to zero as the boundaries are closed until, for Case V, the mean correction factor is approximately that desired. Also, when the mean values of these curves, throughout the range of lift coefficient, are plotted against percent of closure, the resulting curve is smooth within the limits of experimental accuracy. This is certainly not the case with the angle of attack correction factors of Fig. 15. Here, although the relative similarities of the variation with lift coefficient are more pronounced than for the drag correction factor curves, the tendency of the mean or integrated value is to change from negative for Case I to positive for Case II, back to negative for Case III and thence to increase positively to the values of Cases IV,V, and VI. It was for this reason that the percent of closure for Case V was selected on the basis of zero drag correction factors rather than on an average of the values of δ_D and δ_α. It does not seem possible that the behavior of this final angle of attack correction factor curve can be explained either by experimental error or by the blocking effect and change in "q" to which Theodorsen attributed the discrepancies of his experimental results.

In obtaining "free air" curves of C_D and α versus lift coefficient averages were made of the results from tests in the open and closed tunnels. The total increments between these curves gave mean values for δ_D of $\pm.151$ and for δ_α of $\pm.121$ as shown in Table XVII. These results were quite satisfactory when compared with the theoretical computations presented to-date, although the error in relative magnitudes is present here also.

In their last reports on this subject Glauert and Theodorsen have presented theoretical correction factors which show the variation with the ratio of span to tunnel width in a square tunnel. These factors are as follows:

Ratio: $\frac{\text{span}}{\text{tunnel width}}$ =	.4	= .6	= .8
	12"airfoil	18"airfoil	24"airfoil
Theodorsen-			
Open tunnel (Ref.7)	-.1375	-.139	-.151
Closed tunnel (Ref.16)	+.140	+.152	+.180
Glauert-			
Closed tunnel $\delta(U)$	+.142	+.1525	+.181
Closed tunnel $\delta(E)$	+.1405	+.1475	+.1635

Therefore, using Glauert's $\delta(U)$ for the closed tunnel, computed for uniform lift distribution over the 18" airfoil, and Theodorsen's δ for the open tunnel, we obtain an average of .146. Either value varies from the average by 4.8 percent. Likewise, for the 12" airfoil, the error in using the average value instead of the theoretical value is 1.65 percent, and for the 24" airfoil, the error is 7.9 percent. For all results obtained in this report, as has been mentioned previously, averages of open and closed results have been used for free air conditions. This is correct within the limits of experimental accuracy, especially for the case of the 12" airfoil or wing of aspect ratio 4.

However, as shown by Table XVII and Figs. 13 and 16, this is the case for which the experimental values of δ_D and δ_α break down the most. It is to be noted that the force tests on the 12" airfoil were made in the tunnel surrounded by the slotted jet boundaries which approximated free air conditions for the drag values of the 18" airfoil - Case V. Theoretically, as the ratio of span to tunnel width is decreased, the correction factor should be decreased. But, according to experimental results, as the ratio is decreased, the correction factor increases in magnitude and remains of the same sign, and as the ratio increases to .8 (for the 24" airfoil), the correction factor decreases in value. The results of the force tests for the 12" and 18" airfoils are not plotted in the final curve of Fig. 5, as they are definitely not consistent with the theory. The significance of their behavior is again unknown at present.

Conclusions

Although the results of these tests were not altogether satisfactory from the viewpoint with which the problem was originally attacked, some conclusions may be made, as follows:

1. A tunnel of square cross-section, having a boundary about all four sides with a number of symmetrical longitudinal openings, must be almost completely (approximately 95 percent) closed in order to simulate free air conditions with respect to drag.

2. The correction factor for angle of attack does not vary with amount of opening in the same way as does the drag correction factor. The drag factor varies approximately logarithmically, but the angle of attack variation seems to be sinusoidal with percent of closure. From these results, it may be possible to obtain three different slat/slot ratios, *for boundaries about a square tunnel, that will simulate free* air conditions, with respect to angle of attack.

3. Variation of span/tunnel width ratios produces an effect on the correction factors opposite to that expected from the theory. That is, the correction factors have appeared to increase in magnitude when the span is decreased, the tunnel width remaining constant.

4. It may also be mentioned in conclusion that, although it was possible with this apparatus to obtain results only for a jet of square section, it may be possible that similar or more consistent results could be obtained for other practical

shapes of jets. Investigations of other types of jet boundaries containing other arrangements of openings (such as boundaries of wire mesh, vertically slotted boundaries, or solid boundaries having single symmetrically placed openings), might be made with more success, the purpose being to construct and test a system of jet boundaries which, if applied to any practical shape of jet, will produce equally consistent results.

REFERENCES AND BIBLIOGRAPHY

1. Prandtl, L.: Application of Modern Hydrodynamics to Aeronautics. N.A.C.A. Technical Report No.116, 1921, Part II, E and F.

2. Glauert, H.: Aerofoil Theory. A.R.C. Reports and Memoranda No.723, 1920, in A.R.C. Annual Report 1920-21, v.1, p.175-177.

3. Glauert, H.: The Interference of Wind Channel Walls on the Aerodynamic Characteristics of an Aerofoil. A.R.C. Reports and Memoranda No.867, 1923, in A.R.C. Annual Report 1923-24, v.1, p.118-124.

4. Terazawa, K.: On the Interference of Wind Tunnel Walls of Rectangular Cross-Section on the Aerodynamical Characteristics of a Wing. Aeronautical Research Institute, Tokyo Imperial Univ. Report No.44, 1928.

5. Rosenhead, L.: The Effect of Wind Tunnel Interference on the Characteristics of an Aerofoil. Royal Society of London Proceedings, (A), Sept.-Nov.1930, v.129, p.135-145.

6. Theodorsen, T.: The Theory of Wind Tunnel Wall Interference. N.A.C.A. Technical Report No.410, 1931.

7. Theodorsen, T.: Interference of an Airfoil of Finite Span in an Open Rectangular Wind Tunnel. N.A.C.A. Technical Report No.461, 1933.

8. Sanuki, M. and Tani, I.: The Wall Interference of a Wind Tunnel of Elliptic Cross-Section. Proceedings Phys. Math. Soc. of Japan, v.14, no.10, 3rd Series, 1932, p.592.

9. Rosenhead, L.: The Aerofoil in a Wind Tunnel of Elliptic Section. Royal Society of London Proceedings, (A), April-June, 1933, v.140, p.579-604.

10. Glauert, H.: Wind Tunnel Interference on Wings, Bodies and Airscrews. A.R.C. Reports and Memoranda No.1566. Pt.I and II. 1933.

11. Cowley, W.L. and Jones, L.J.: An Experimental Test of the Prandtl Correction for Tunnel Wall Interference. A.R.C. Reports and Memoranda No.898, 1924, in A.R.C. Annual Report 1923-24, v.2, p.538-541.

12. Higgins, G.J.: Wall Interference in Closed Type Wind Tunnels. N.A.C.A. Technical Notes No.256, 1927.

13. Higgins, G.J.: The Effect of the Walls in Closed Type Wind Tunnels . N.A.C.A.Technical Report No.275, 1927.

14. Knight, Montgomery and Harris, T.A.: Experimental Determination of Jet Boundary Corrections for Airfoil Tests in Four Open Wind Tunnel Jets of Different Shapes. N.A.C.A.Technical Report No.361, 1930.

15. Glauert, H.: The Elements of Aerofoil and Airscrew Theory. Cambridge Univ.Press, 1926 and 1930, Chap.XIV, 2nd ed.

16. Theodorsen, T.: Experimental Verification of the Theory of Wind Tunnel Boundary Interference. N.A.C.A.Technical Report No.478, 1934.

17. Schliestett, G.V.: Experimental Verification of Theodorsen's Theoretical Jet Boundary Correction Factors. N.A.C.A.Technical Notes No.506, 1934.

Glauert,H. and Hartshorn, A.S.: The Interference of Wind Channel Walls on the Downwash Angle and Tail-Setting to Trim. A.R.C.Reports and Memoranda No.947, 1924, in A.R.C.Annual Report 1924-25, v.1, p.83-91.

Sasaki, T.: On the Effect of the Wall of a Wind Tunnel upon the Lift Coefficient of a Model. Aero. Research Institute, Tokyo Imperial Univ. Report No.46, 1928.

Glauert, H.: The Interference on the Characteristics of an Aerofoil in a Wind Tunnel of Circular Section. A.R.C.Reports and Memoranda No.1453, 1931, in A.R.C. Annual Report 1932-33, v.1, p.229-240.

Glauert, H.: The Interference on the Characteristics of an Aerofoil in a Wind Tunnel of Rectangular Section. A.R.C.Reports and Memoranda No.1459, 1932, in A.R.C. Annual Report 1932-33, v.1, p.241-247.

Glauert, H.: Some General Theorems Concerning Wind Tunnel Interference on Aerofoils. A.R.C.Reports and Memoranda No.1470, 1932, in A.R.C.Annual Report, 1932-33, v.1, p.218-228.

Seiferth, R.: Experiments on Aircraft Models in the Wind Tunnel. Handbook of Experimental Physics. 1932, v.4, Pt.2, p.162.

Rosenhead, L.: Interference Due to the Walls of a Wind Tunnel. Royal Society of London Proceedings, (A), Oct.-Nov., 1933, v.142, p.308-320.

TABLE I - EXPERIMENTAL δ_D

CASE I - 3" x 18" Clark Y Airfoil

Open Jet

C_L	C_D''	C_D'	C_D	ΔC_D	δ_D
0.0	.0186	.0186	.0186	.0000	
.1	.0176	.0176	.0173	-.0003	-.602
.2	.0182	.0182	.0174	-.0008	-.344
.3	.0205	.0205	.0191	-.0014	-.267
.4	.0242	.0242	.0224	-.0018	-.199
.5	.0302	.0302	.0275	-.0027	-.185
.6	.0377	.0377	.0344	-.0033	-.157
.7	.0467	.0467	.0426	-.0041	-.146
.8	.0573	.0573	.0523	-.0050	-.136
.9	.0693	.0693	.0635	-.0058	-.123
.95	.0779	.0779	.0707	-.0072	-.137
1.0	.0871	.0871	.0794	-.0077	-.132
1.05	.0993	.0993	.0914	-.0079	-.124

Mean δ_D integrated from C_L = .4 to C_L = 1.05: -.151

TABLE II - EXPERIMENTAL δ_α

CASE I - 3" x 18" Clark Y Airfoil

Open Jet

C_L	α'	α	$\Delta\alpha$	δ_α
0.0	0.00	0.00	.00	
.1	1.39	1.34	-.06	-.165
.2	2.83	2.73	-.11	-.157
.3	4.28	4.15	-.14	-.135
.4	5.76	5.60	-.17	-.124
.5	7.27	7.06	-.22	-.129
.6	8.76	8.54	-.23	-.112
.7	10.28	10.03	-.26	-.109
.8	11.87	11.57	-.31	-.114
.9	13.51	13.14	-.37	-.123
.95	14.41	14.00	-.42	-.131
1.0	15.43	15.06	-.38	-.112
1.05	16.78	16.51	-.28	-.079

Mean δ_α integrated from C_L = .2 to C_L = 1.05: -.121

TABLE III - EXPERIMENTAL δ_D

CASE II - 3" x 18" Clark Y Airfoil

50 Percent Closed Jet

C_L	C_D''	C_D'	C_D	ΔC_D	δ_D
0.0	.0196	.0186	.0186	.0000	
.1	.0186	.0176	.0173	-.0003	-.515
.2	.0192	.0182	.0174	-.0008	-.344
.3	.0212	.0202	.0191	-.0011	-.210
.4	.0246	.0236	.0224	-.0012	-.129
.5	.0301	.0291	.0275	-.0016	-.110
.6	.0376	.0366	.0344	-.0022	-.105
.7	.0472	.0462	.0426	-.0036	-.126
.8	.0584	.0574	.0523	-.0051	-.137
.9	.0711	.0701	.0635	-.0066	-.140
.95	.0784	.0774	.0707	-.0067	-.128
1.0	.0868	.0858	.0794	-.0064	-.110
1.05	.0998	.0988	.0914	-.0074	-.115

Mean δ_D integrated from C_L = .4 to C_L = 1.05: -.124

TABLE IV - EXPERIMENTAL δ_α

CASE II - 3" x 18" Clark Y Airfoil

50 Percent Closed Jet

C_L	α'	α	$\Delta\alpha$	δ_α
0.0	0.00	0.00	.00	
.1	1.33	1.34	+.01	+.015
.2	2.69	2.73	+.04	+.053
.3	4.07	4.15	+.08	+.075
.4	5.46	5.60	+.14	+.101
.5	6.87	7.06	+.19	+.111
.6	8.28	8.54	+.26	+.127
.7	9.74	10.03	+.29	+.122
.8	11.30	11.57	+.27	+.099
.9	12.99	13.14	+.15	+.050
.95	13.92	14.00	+.08	+.024
1.0	14.95	15.06	+.11	+.032
1.05	16.12	16.51	+.39	+.110

Mean δ_α integrated from C_L = .1 to C_L = 1.05: +.085

TABLE V - EXPERIMENTAL δ_D

CASE III - 3" x 18" Clark Y Airfoil

67 Percent Closed Jet

C_L	C_D''	C_D'	C_D	ΔC_D	δ_D
0.0	.0186	.0186	.0186	.0000	
.1	.0178	.0178	.0173	-.0005	-.859
.2	.0184	.0184	.0174	-.0010	-.430
.3	.0207	.0207	.0191	-.0016	-.305
.4	.0245	.0245	.0224	-.0021	-.226
.5	.0298	.0298	.0275	-.0023	-.158
.6	.0371	.0371	.0344	-.0027	-.129
.7	.0464	.0464	.0426	-.0038	-.133
.8	.0573	.0573	.0523	-.0050	-.134
.9	.0698	.0698	.0635	-.0063	-.134
.95	.0767	.0767	.0707	-.0060	-.114
1.0	.0854	.0854	.0794	-.0060	-.103
1.05	.0972	.0972	.0914	-.0058	-.090

Mean δ_D integrated from C_L = .5 to C_L = 1.05: -.129

TABLE VI - EXPERIMENTAL δ_α

CASE III - 3" x 18" Clark Y Airfoil

67 Percent Closed Jet

C_L	α'	α	$\Delta\alpha$	δ_α
0.0	0.00	0.00	.00	
.1	1.37	1.34	-.04	-.105
.2	2.76	2.73	-.04	-.053
.3	4.17	4.15	-.03	-.025
.4	5.59	5.60	+.01	+.004
.5	7.03	7.06	+.03	+.015
.6	8.51	8.54	+.03	+.013
.7	9.98	10.03	+.05	+.019
.8	11.53	11.57	+.04	+.013
.9	13.18	13.14	-.04	-.013
.95	14.03	14.00	-.04	-.011
1.0	15.01	15.06	+.05	+.014
1.05	16.18	16.51	+.33	+.093

Mean δ_α integrated from C_L = .1 to C_L = 1.05: -.009

TABLE VII - EXPERIMENTAL δ_D

CASE IV - 3" x 18" Clark Y Airfoil

83 Percent Closed Jet

C_L	C_D''	C_D'	C_D	ΔC_D	δ_D
0.0	.0175	.0186	.0186	.0000	
.1	.0168	.0179	.0173	-.0006	-1.031
.2	.0177	.0188	.0174	-.0014	- .602
.3	.0199	.0210	.0191	-.0019	- .363
.4	.0234	.0245	.0224	-.0021	- .226
.5	.0286	.0297	.0275	-.0022	- .151
.6	.0355	.0366	.0344	-.0022	- .105
.7	.0442	.0453	.0426	-.0027	- .095
.8	.0544	.0555	.0523	-.0032	- .086
.9	.0658	.0669	.0635	-.0034	- .072
.95	.0734	.0745	.0707	-.0038	- .072
1.0	.0816	.0827	.0794	-.0033	- .057
1.05	.0923	.0934	.0914	-.0020	- .031

Mean δ_D integrated from C_L = .5 to C_L = 1.05: -.088

TABLE VIII - EXPERIMENTAL δ_α

CASE IV - 3" x 18" Clark Y Airfoil

83 Percent Closed Jet

C_L	α'	α	$\Delta\alpha$	δ_α
0.0	0.00	0.00	.00	
.1	1.31	1.34	+.03	+.075
.2	2.65	2.73	+.08	+.112
.3	4.01	4.15	+.14	+.135
.4	5.40	5.60	+.20	+.146
.5	6.79	7.06	+.27	+.159
.6	8.21	8.54	+.33	+.162
.7	9.62	10.03	+.41	+.174
.8	11.13	11.57	+.44	+.163
.9	12.77	13.14	+.37	+.123
.95	13.64	14.00	+.36	+.109
1.0	14.60	15.06	+.46	+.136
1.05	16.17	16.51	+.34	+.096

Mean δ_α integrated from C_L = .1 to C_L = 1.05: +.138

TABLE IX - EXPERIMENTAL δ_D

CASE VI - 3" x 18" Clark Y Airfoil

Closed Jet

C_L	C_D''	C_D'	C_D	ΔC_D	δ_D
0.0	.0186	.0186	.0186	.0000	
.1	.0169	.0169	.0173	+.0003	+.602
.2	.0166	.0166	.0174	+.0008	+.344
.3	.0177	.0177	.0191	+.0014	+.267
.4	.0205	.0205	.0224	+.0018	+.199
.5	.0248	.0248	.0275	+.0027	+.185
.6	.0311	.0311	.0344	+.0033	+.157
.7	.0384	.0384	.0426	+.0041	+.146
.8	.0472	.0472	.0523	+.0050	+.136
.9	.0577	.0577	.0635	+.0058	+.123
.95	.0635	.0635	.0707	+.0072	+.137
1.0	.0717	.0717	.0794	+.0077	+.132
1.05	.0834	.0834	.0914	+.0079	+.124

Mean δ_D integrated from C_L = .4 to C_L = 1.05: +.151

TABLE X - EXPERIMENTAL δ_α

CASE VI - 3" x 18" Clark Y Airfoil

Closed Jet

C_L	α'	α	$\Delta\alpha$	δ_α
0.0	0.00	0.00	.00	
.1	1.28	1.34	+.06	+.165
.2	2.62	2.73	+.11	+.157
.3	4.01	4.15	+.14	+.135
.4	5.43	5.60	+.17	+.124
.5	6.84	7.06	+.22	+.129
.6	8.31	8.54	+.23	+.112
.7	9.77	10.03	+.26	+.109
.8	11.26	11.57	+.31	+.114
.9	12.77	13.14	+.37	+.123
.95	13.58	14.00	+.42	+.131
1.0	14.68	15.06	+.38	+.112
1.05	16.23	16.51	+.28	+.079

Mean δ_α integrated from C_L = .2 to C_L = 1.05: +.121

TABLE XI - EXPERIMENTAL δ_D

CASE V - 3" x 18" Clark Y Airfoil

93.1 Percent Closed Jet

C_L	C_D''	C_D'	C_D	ΔC_D	δ_D
0.0	.0208	.0186	.0186	.0000	
.1	.0195	.0173	.0173	.0000	.000
.2	.0195	.0173	.0174	+.0001	+.043
.3	.0213	.0191	.0191	.0000	.000
.4	.0250	.0228	.0224	-.0004	-.043
.5	.0302	.0280	.0275	-.0005	-.034
.6	.0370	.0348	.0344	-.0004	-.019
.7	.0454	.0432	.0426	-.0006	-.021
.8	.0558	.0536	.0523	-.0013	-.035
.9	.0686	.0664	.0635	-.0029	-.062
.95	.0762	.0740	.0707	-.0033	-.063
1.0	.0849	.0827	.0794	-.0033	-.057
1.05	.0953	.0931	.0914	-.0017	-.026

Mean δ_D integrated from $C_L = .2$ to $C_L = 1.05$: -.031

TABLE XII - EXPERIMENTAL δ_α

CASE V - 3" x 18" Clark Y Airfoil

93.1 Percent Closed Jet

C_L	α'	α	$\Delta\alpha$	δ_α
0.0	0.00	0.00	.00	
.1	1.33	1.34	+.01	+.015
.2	2.67	2.73	+.06	+.083
.3	4.03	4.15	+.12	+.115
.4	5.41	5.60	+.19	+.138
.5	6.79	7.06	+.27	+.159
.6	8.19	8.54	+.35	+.172
.7	9.63	10.03	+.40	+.169
.8	11.18	11.57	+.39	+.144
.9	12.88	13.14	+.26	+.087
.95	13.87	14.00	+.13	+.040
1.0	14.92	15.06	+.14	+.041
1.05	16.23	16.51	+.28	+.079

Mean δ_α integrated from $C_L = .1$ to $C_L = 1.05$: +.123

TABLE XIII - EXPERIMENTAL δ_D

CASE V - 3" x 12" Clark Y Airfoil

93.1 Percent Closed Jet

C_L	C_D''	C_D'	C_D	ΔC_D	δ_D
0.0	.0199	.0199	.0199	.0000	
.1	.0187	.0187	.0188	+.0001	+.253
.2	.0201	.0201	.0198	-.0003	-.190
.3	.0239	.0239	.0228	-.0011	-.309
.4	.0301	.0301	.0279	-.0022	-.348
.5	.0388	.0388	.0354	-.0034	-.344
.6	.0492	.0492	.0453	-.0039	-.274
.7	.0615	.0615	.0569	-.0046	-.238
.8	.0769	.0769	.0705	-.0064	-.253
.9	.0946	.0946	.0863	-.0083	-.259
.95	.1040	.1040	.0959	-.0081	-.224
1.0	.1150	.1150	.1072	-.0078	-.198
1.05	.1293	.1293	.1219	-.0074	-.170

Mean δ_D integrated from C_L = .2 to C_L = 1.05: -.270

TABLE XIV - EXPERIMENTAL δ_α

CASE V - 3" x 12" Clark Y Airfoil

93.1 Percent Closed Jet

C_L	α'	α	$\Delta\alpha$-	δ_α
0.0	0.00	0.00	.00	
.1	1.56	1.48	-.07	-.323
.2	3.14	3.03	-.11	-.245
.3	4.74	4.60	-.14	-.205
.4	6.38	6.20	-.18	-.196
.5	8.03	7.82	-.22	-.190
.6	9.71	9.45	-.26	-.194
.7	11.42	11.09	-.33	-.209
.8	13.17	12.78	-.39	-.215
.9	15.04	14.51	-.53	-.261
.95	16.08	15.44	-.64	-.298
1.0	17.24	16.58	-.67	-.294
1.05	18.54	18.10	-.44	-.185

Mean δ_α integrated from C_L = .1 to C_L = 1.05: -.223

TABLE XV - EXPERIMENTAL δ_D

CASE V - 3" x 24" Clark Y Airfoil

93.1 Percent Closed Jet

C_L	C_D''	C_D'	C_D	ΔC_D	δ_D
0.0	.0183	.0183	.0183	.0000	
.1	.0167	.0167	.0168	+.0001	+.127
.2	.0168	.0168	.0166	-.0002	-.064
.3	.0183	.0183	.0177	-.0006	-.085
.4	.0211	.0211	.0200	-.0011	-.087
.5	.0254	.0254	.0240	-.0014	-.071
.6	.0310	.0310	.0295	-.0015	-.053
.7	.0376	.0376	.0360	-.0016	-.042
.8	.0455	.0455	.0438	-.0017	-.034
.9	.0548	.0548	.0529	-.0019	-.030
.95	.0601	.0601	.0590	-.0011	-.016
1.0	.0661	.0661	.0664	+.0003	+.004
1.05	.0728	.0728	.0771	+.0043	+.050

Mean δ_D integrated from C_L = .1 to C_L = 1.05: -.047

TABLE XVI - EXPERIMENTAL δ_α

CASE V - 3" x 24" Clark Y Airfoil

93.1 Percent Closed Jet

C_L	α'	α	$\Delta\alpha$	δ_α
0.0	0.00	0.00	.00	
.1	1.22	1.26	+.04	+.093
.2	2.46	2.58	+.12	+.133
.3	3.72	3.93	+.21	+.153
.4	4.98	5.30	+.32	+.180
.5	6.27	6.69	+.42	+.187
.6	7.58	8.10	+.52	+.192
.7	8.92	9.52	+.60	+.189
.8	10.32	10.98	+.66	+.184
.9	11.81	12.49	+.68	+.167
.95	12.61	13.31	+.70	+.162
1.0	13.47	14.33	+.86	+.191
1.05	14.44	15.74	+1.30	+.275

Mean δ_α integrated from C_L = .1 to C_L = 1.05: +.177

TABLE XVII - SUMMARY

Mean Integrated Values of Correction Factors

		δ_D	δ_α
CASE I	- Open Jet - 3"x18"	-.151	-.121
CASE II	- 50.0 Percent Closed Jet - 3"x18"	-.124	+.085
CASE III	- 66.7 Percent Closed Jet - 3"x18"	-.129	-.009
CASE IV	- 83.3 Percent Closed Jet - 3"x18"	-.088	+.138
CASE V	- 93.1 Percent Closed Jet - 3"x18"	-.031	+.123
CASE VI	- Closed Jet - 3"x18"	+.151	+.121
CASE V	- 93.1 Percent Closed Jet - 3"x12"	-.270	-.223
	- 93.1 Percent Closed Jet - 3"x24"	-.047	+.177

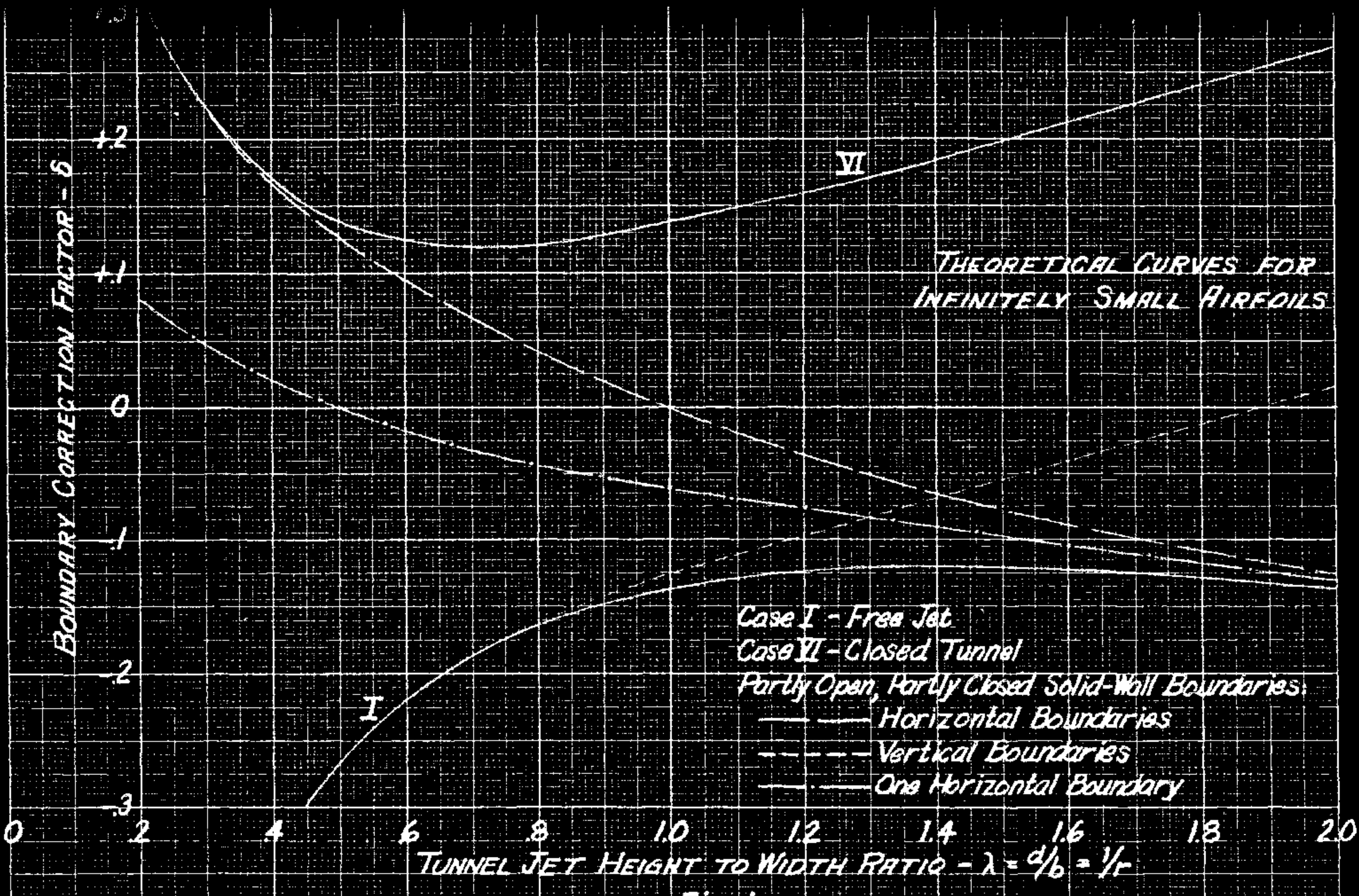
THEORETICAL CURVES FOR
INFINITELY SMALL AIRFOILS
BOUNDARY CORRECTION FACTOR - δ
+.2
+.1
0
-.1
-.2
-.3
0
.2
.4
.6
.8
1.0
1.2
1.4
1.6
1.8
2.0
TUNNEL JET HEIGHT TO WIDTH RATIO - λ = d/b = 1/r
VI
I
Case I - Free Jet
Case VI - Closed Tunnel
Partly Open, Partly Closed Solid-Wall Boundaries:
Horizontal Boundaries
Vertical Boundaries
One Horizontal Boundary

Fig. 1

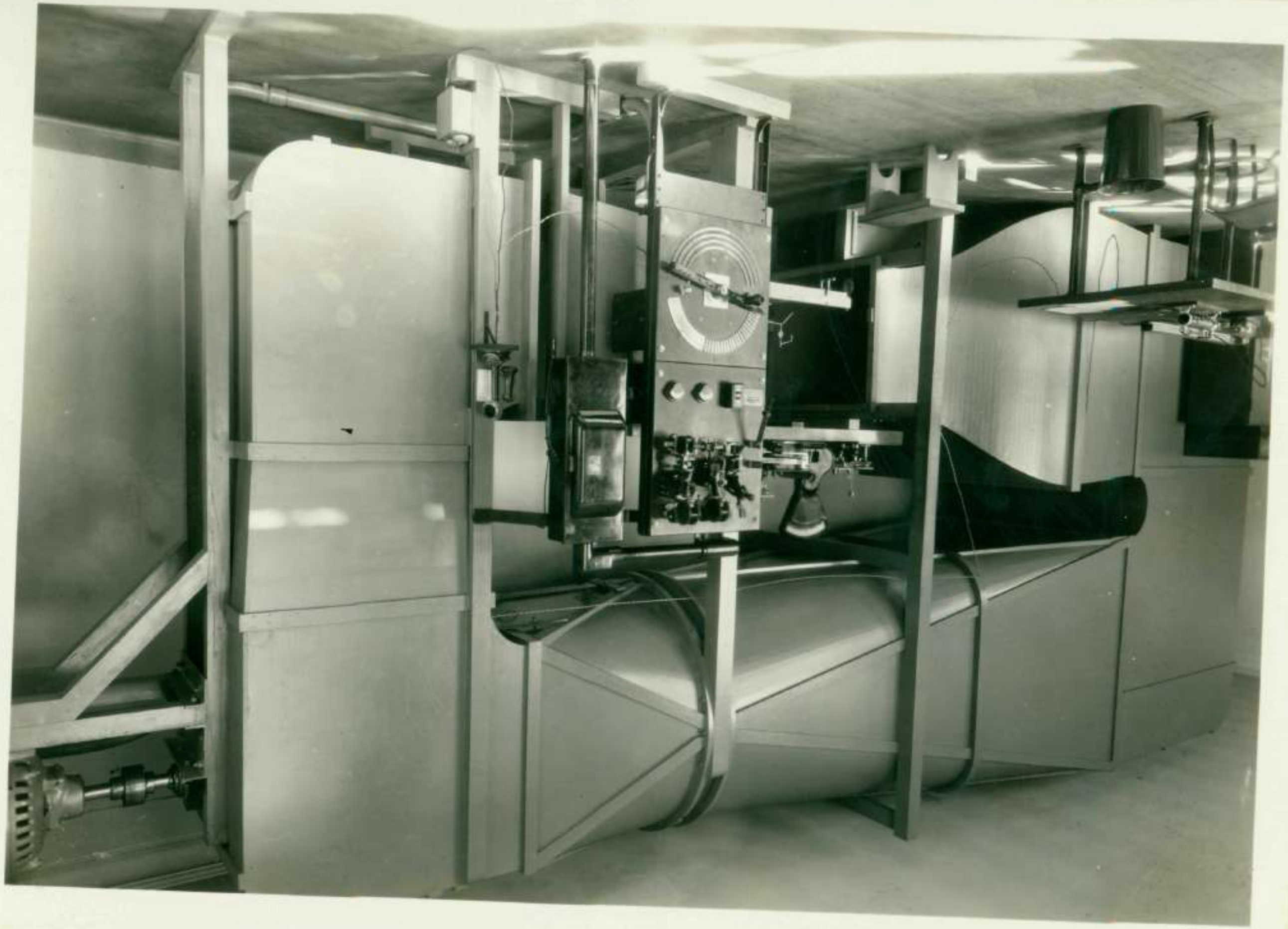

Fig. 2

GEORGIA TECH $2\frac{1}{2}$ FOOT OPEN JET WIND TUNNEL

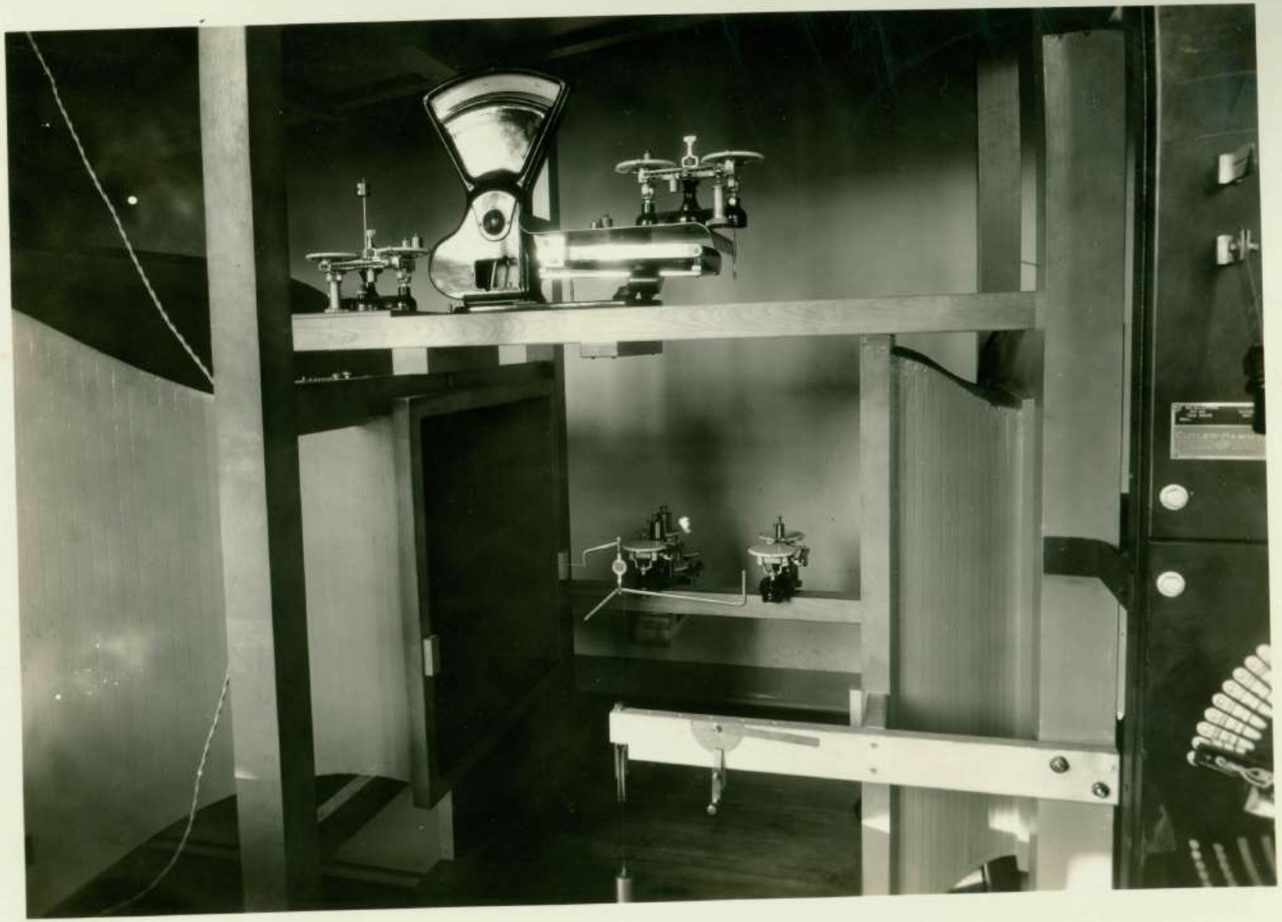

Fig. 3

SIX COMPONENT WIRE BALANCE SYSTEM

Fig. 4

BOUNDARY OF SLOTS AND SLATS - CASE II, 50 PERCENT CLOSED JET

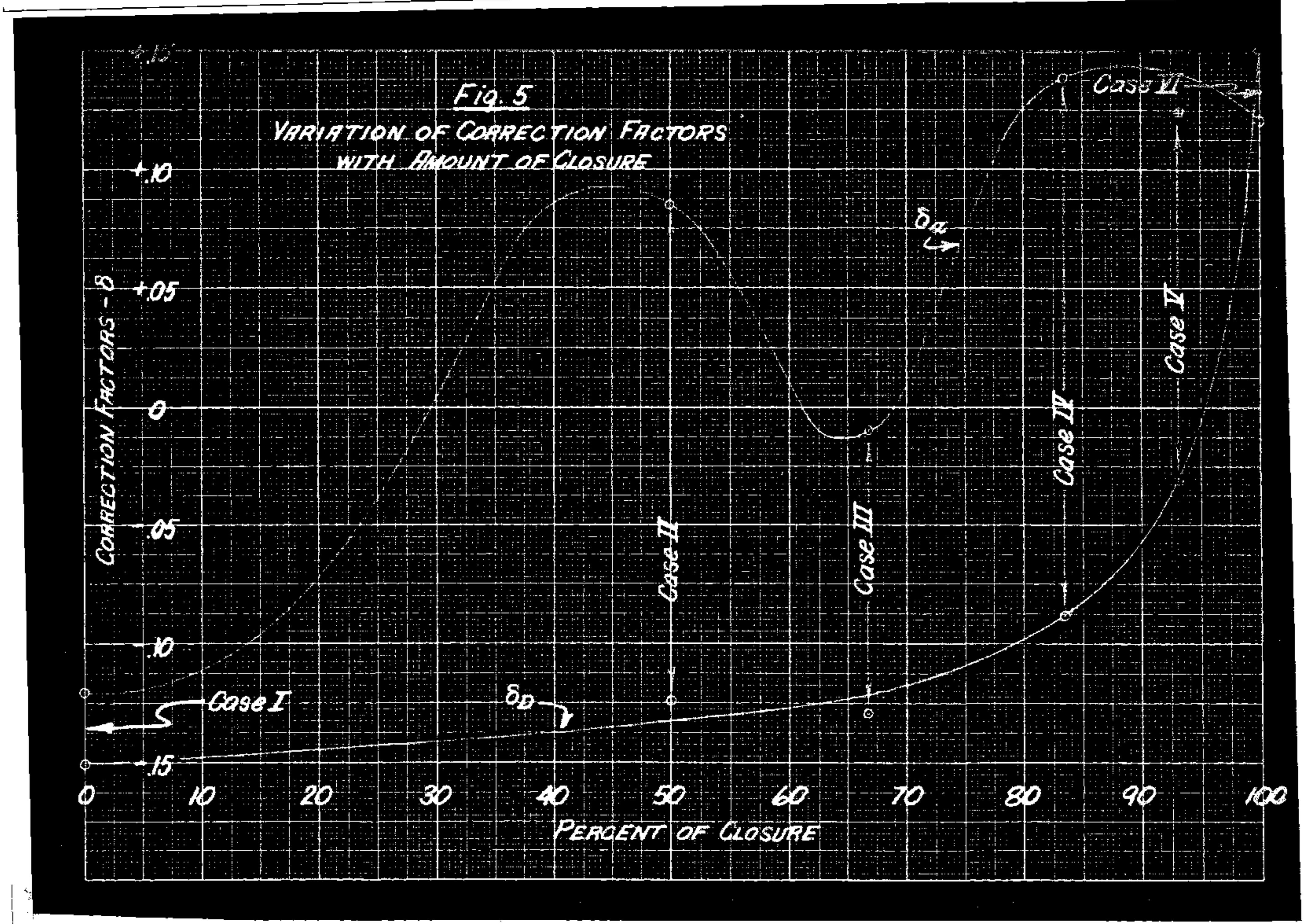
Fig. 5
VARIATION OF CORRECTION FACTORS
WITH AMOUNT OF CLOSURE
CORRECTION FACTORS - δ
PERCENT OF CLOSURE
+.10
+.05
0
-.05
-.10
-.15
0
10
20
30
40
50
60
70
80
90
100
Case I
Case II
Case III
Case IV
Case V
Case VI
δ_a
δ_D

Fig. 6

BOUNDARY OF SLOTS AND SLATS - CASE V, 93.1 PERCENT CLOSED JET

Fig. 7

INTERIOR OF THE TUNNEL JET WITH BOUNDARIES OF CASE V
3" x 24" Airfoil in Place

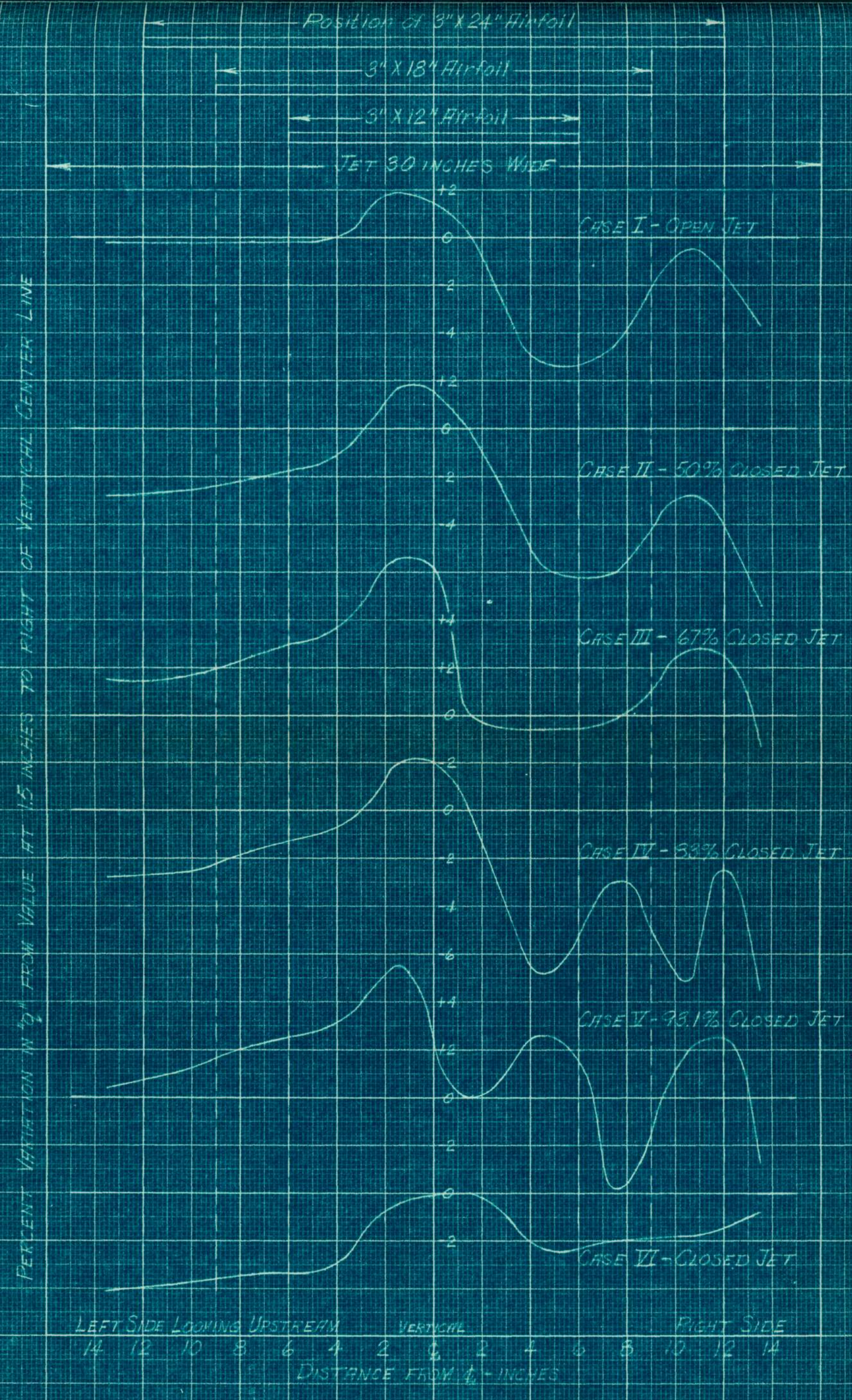

Fig. 8 - Dynamic Pressure Variation over Airfoil Test Region

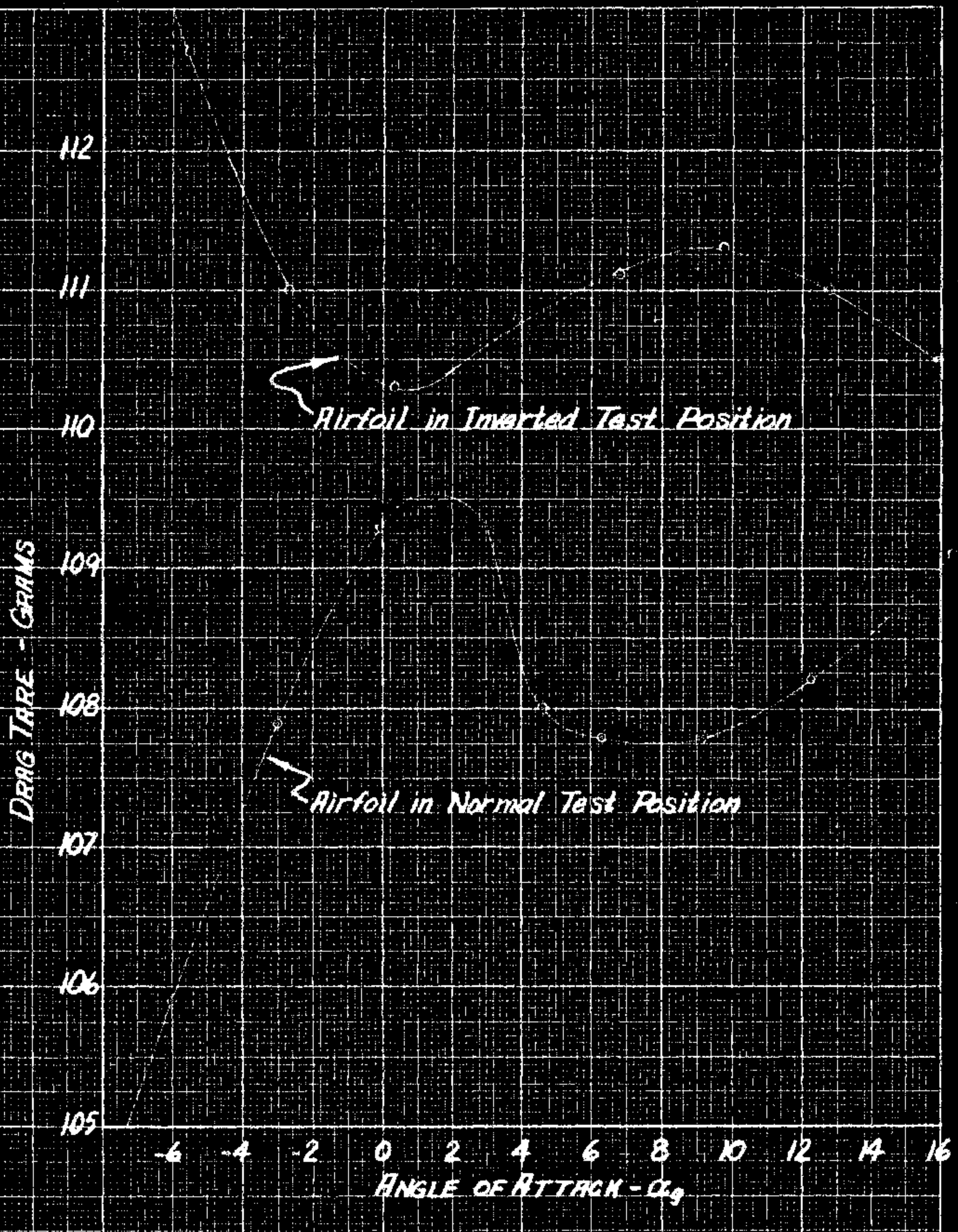

Fig. 9

DYNAMIC TARE FORCES

SIX-COMPONENT BALANCE FRAME

CASE II - TUNNEL 50% CLOSED

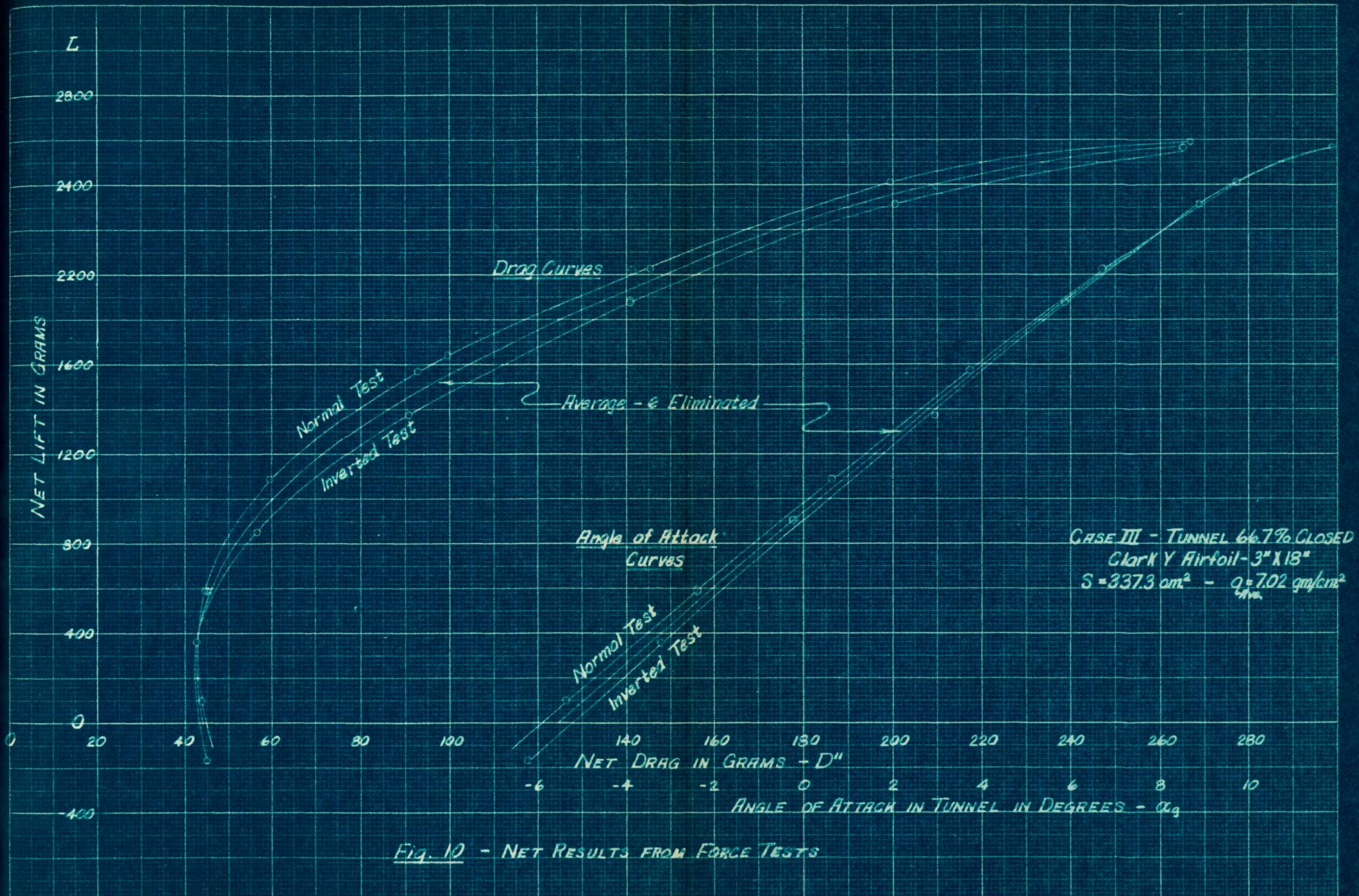

Fig. 10 - Net Results from Force Tests

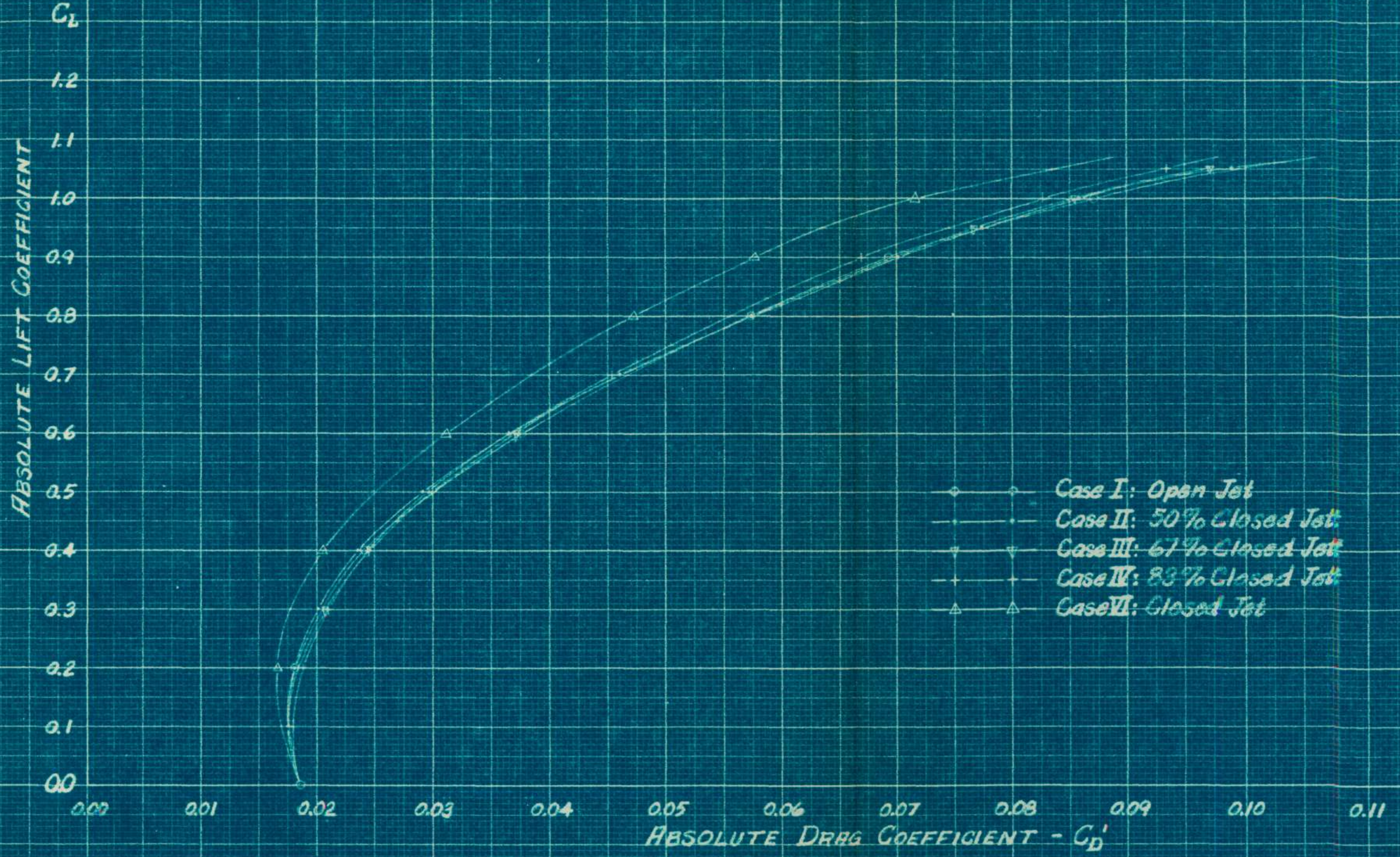

Fig. 11 - Non-Dimensional Adjusted Curves, C_D' vs C_L
Variation with Boundary Closure

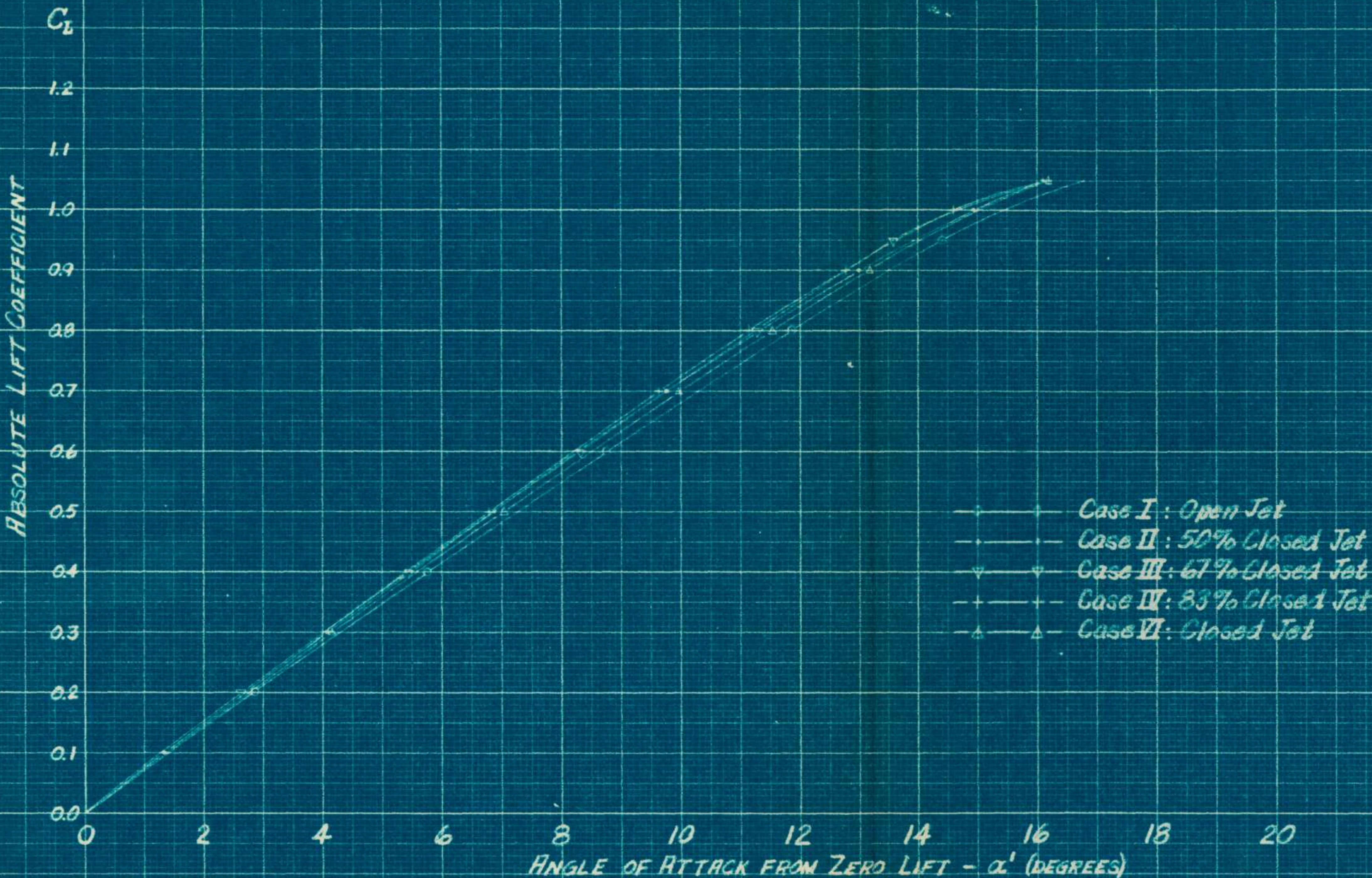

Fig. 12 - Non-Dimensional Adjusted Curves, α' vs C_L
Variation with Boundary Closure

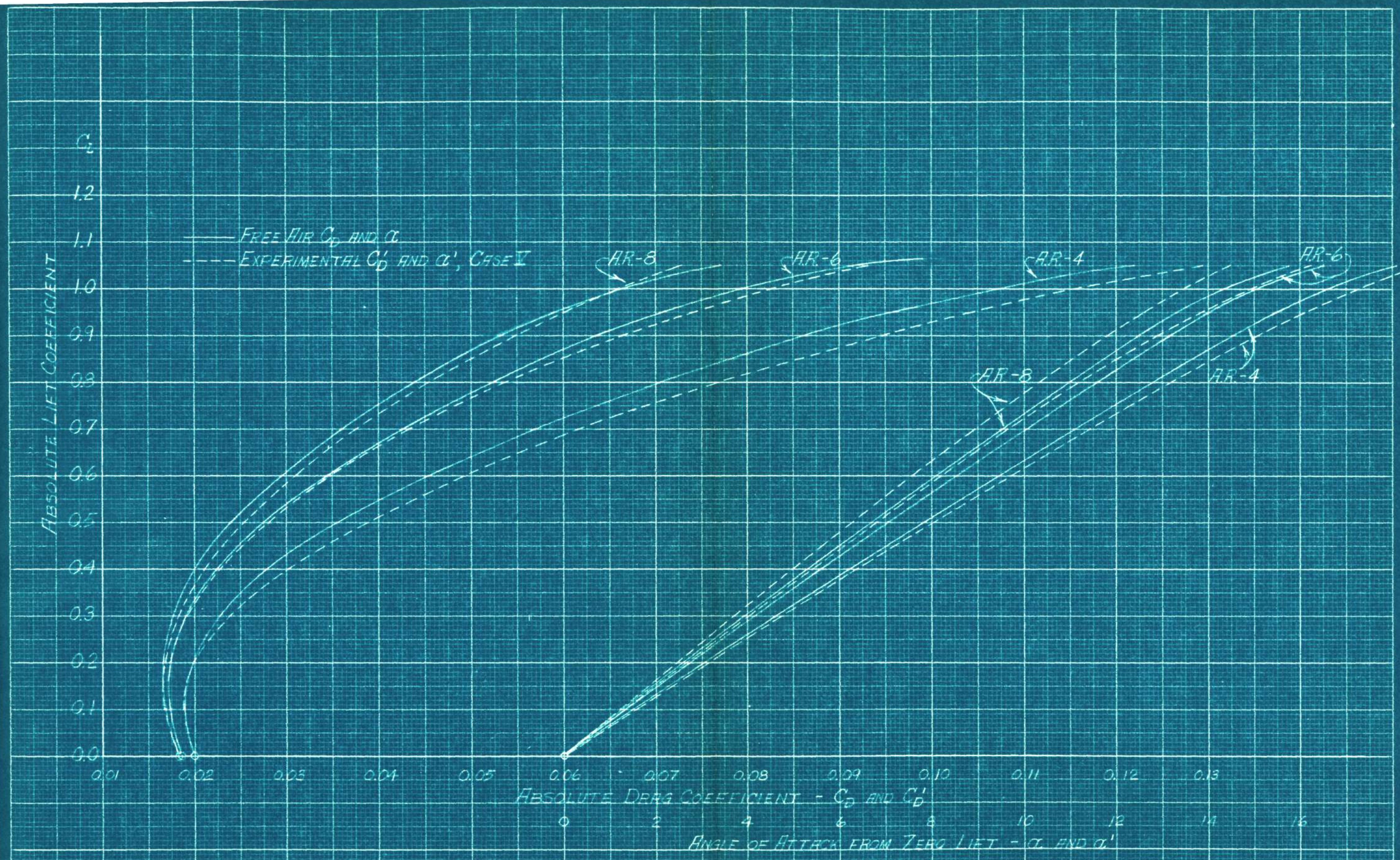

Fig. 13 - Comparison of Final Results for Case V with Free Air Conditions Showing Variation with Aspect Ratio

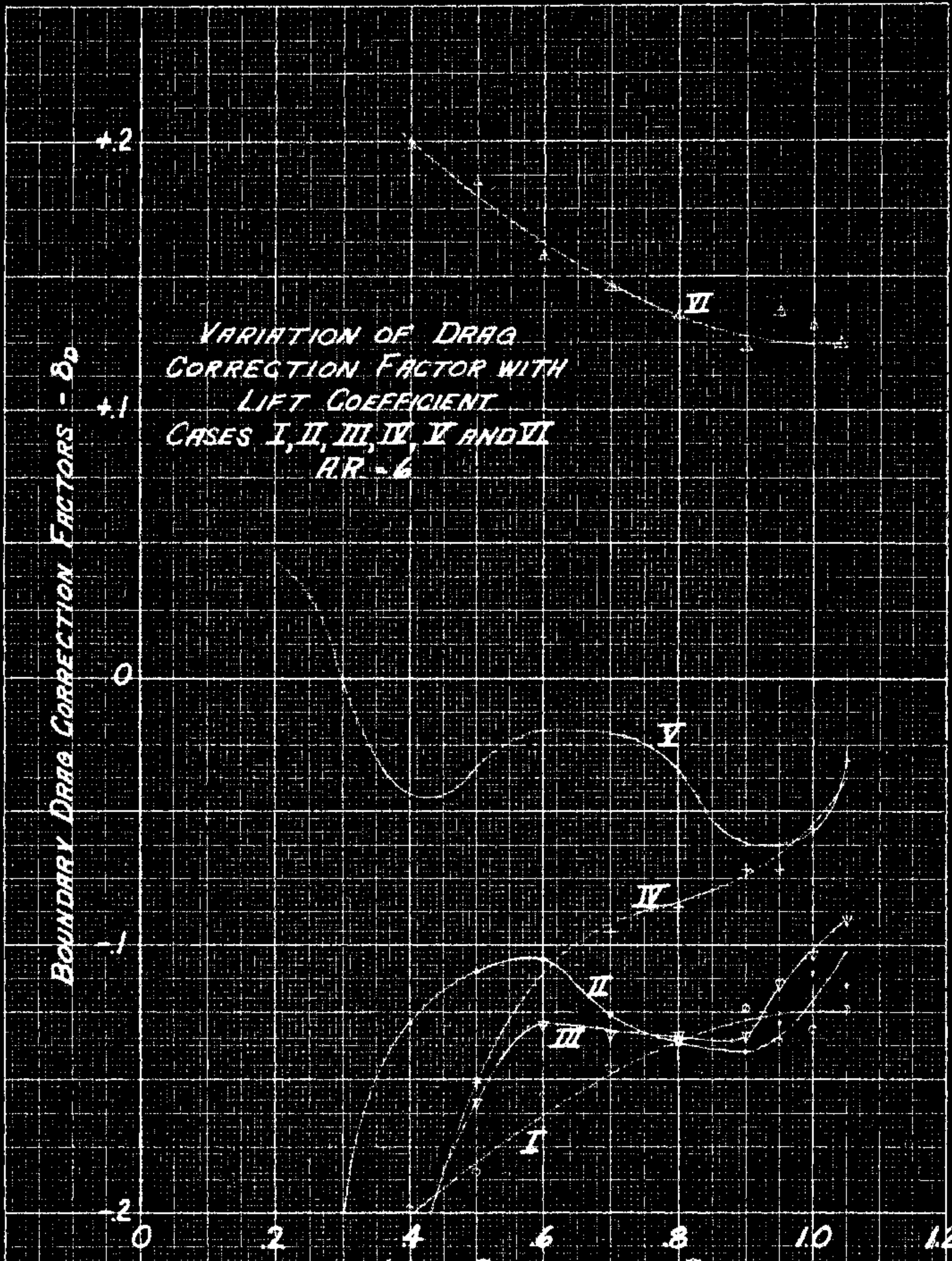

VARIATION OF DRAG
CORRECTION FACTOR WITH
LIFT COEFFICIENT
CASES I, II, III, IV, V AND VI
A.R. - 6
BOUNDARY DRAG CORRECTION FACTORS - δ_D
+.2
+.1
0
-.1
-.2
0
.2
.4
.6
.8
1.0
1.2
I
II
III
IV
V
VI
LIFT COEFFICIENT - C_L

Fig 14

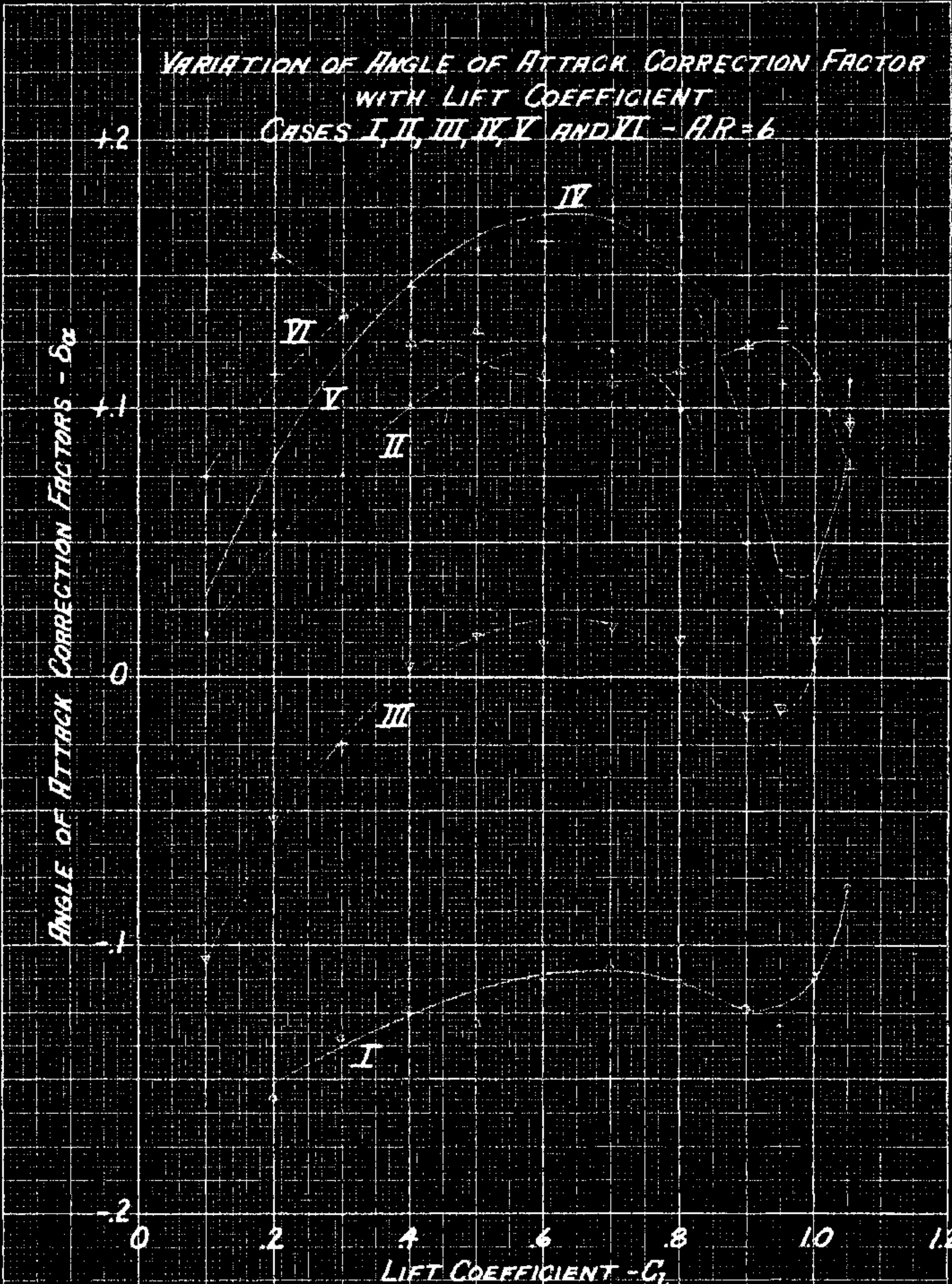
VARIATION OF ANGLE OF ATTACK CORRECTION FACTOR
WITH LIFT COEFFICIENT
CASES I, II, III, IV, V AND VI - A.R.=6
ANGLE OF ATTACK CORRECTION FACTORS - δ_α
+.2
+.1
0
-.1
-.2
0
.2
.4
.6
.8
1.0
1.2
I
II
III
IV
V
VI
LIFT COEFFICIENT - C_L

Fig. 15

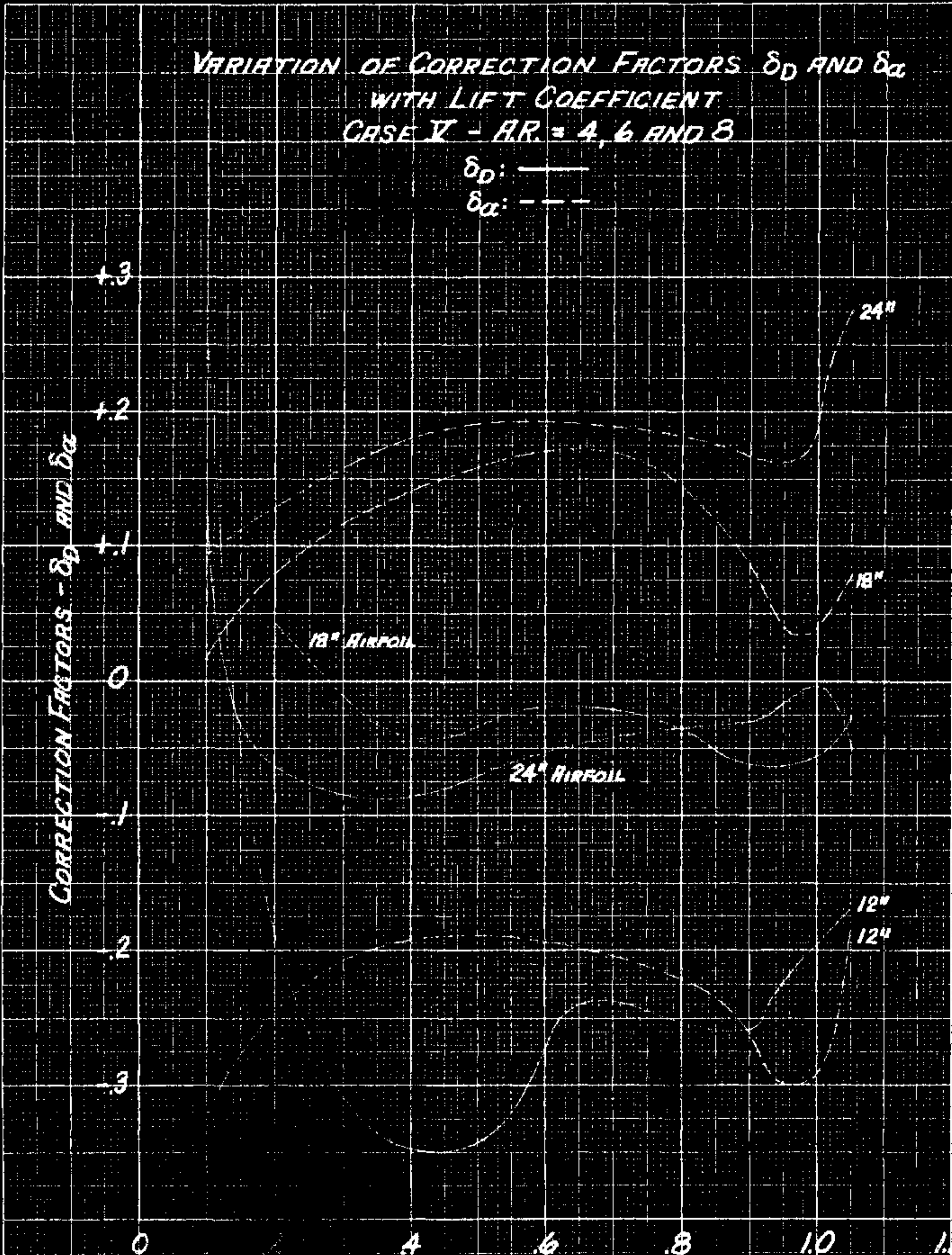
VARIATION OF CORRECTION FACTORS δ_D AND δ_α
WITH LIFT COEFFICIENT
CASE V - A.R. = 4, 6 AND 8
δ_D: ———
δ_α: - - -
+.3
+.2
+.1
0
-.1
-.2
-.3
CORRECTION FACTORS - δ_D AND δ_α
24"
18"
18" AIRFOIL
24" AIRFOIL
12"
12"
0
.2
.4
.6
.8
1.0
1.2
LIFT COEFFICIENT - C_L

Fig. 16